

# 1 Supplementary material for CDS

In what follows, ratios of acceptances are determined as follows: a weight is calculated for each simulated candidate,  $w \equiv 1$  for  $B^0$  decays and  $w \equiv e^{t_{\text{true}}(1/\tau_{B_s^0}^{\text{fs}} - 1/\tau_B)}$  for  $B_s^0$  decays, where  $t_{\text{true}}$  is the true decay time and  $\tau_{B_s^0}^{\text{fs}}$  and  $\tau_B$  are the  $B_{(s)}^0$  lifetimes in simulation; a histogram is filled with the decay time of each candidate weighted with  $w$ ; the ratio of acceptances is the ratio of the histograms.

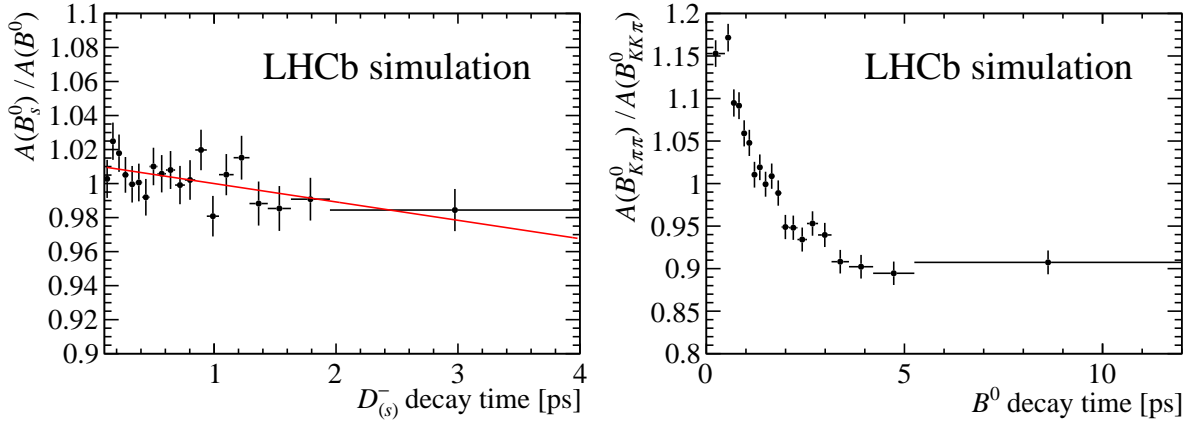


Figure 1: (Left panel) ratio between decay-time acceptances of simulated signal and reference decays as a function of the  $D_{(s)}^-$  decay time. (Right panel) ratio between decay-time acceptances of simulated control and reference decays as a function of the  $B^0$  decay time. A linear fit to the signal-to-reference ratio yields a slope of  $-0.0108 \pm 0.0043 \text{ ps}^{-1}$  with  $\chi^2/\text{ndf} = 14.3/18$  (71%  $p$ -value).

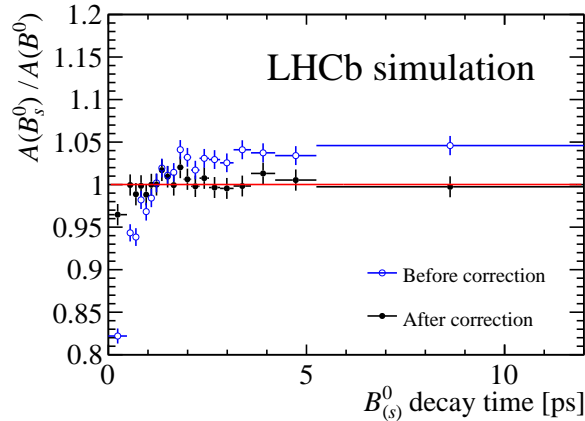


Figure 2: Ratio between decay-time acceptances of simulated signal and reference decays as a function of the  $B_{(s)}^0$  decay time, (open circles) excluding and (full circles) including the correction for differing  $D^-$  and  $D_s^-$  lifetimes. A fit with a constant function is overlaid on the corrected-ratio data, which are compatible with a uniform distribution with  $\chi^2/\text{ndf} = 13.2/18$  (83%  $p$ -value).

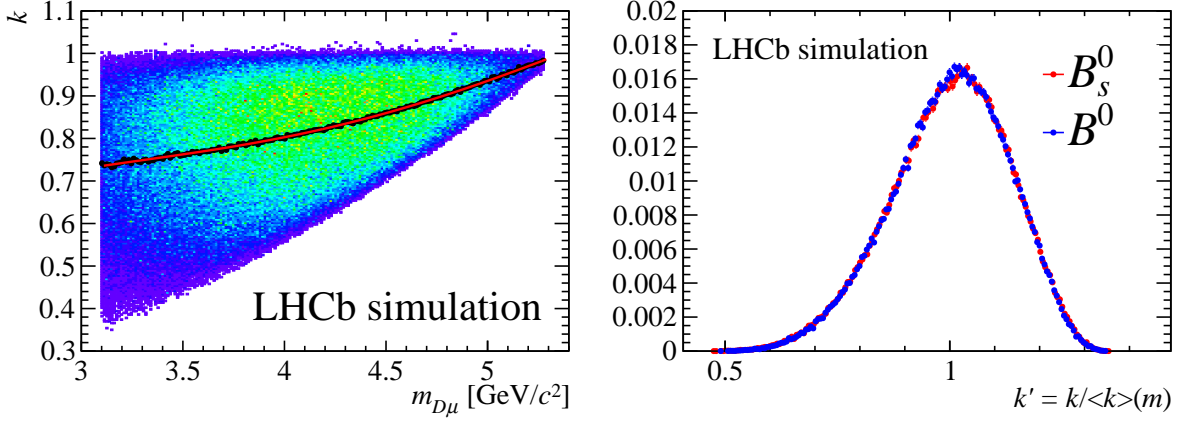


Figure 3: (Left panel) distribution of  $k$ -factor as a function of  $D_s^- \mu^+$  mass for simulated signal decays. The corresponding mean value as a function of  $m_{D\mu}$ ,  $\langle k \rangle(m_{D\mu})$ , is represented by black markers, with a fit to an empirical function overlaid in red. (Right panel) distribution of  $k$ -factor for simulated signal and reference decays. The  $k$ -factors in the latter distributions are scaled to their mean value for presentation purposes.

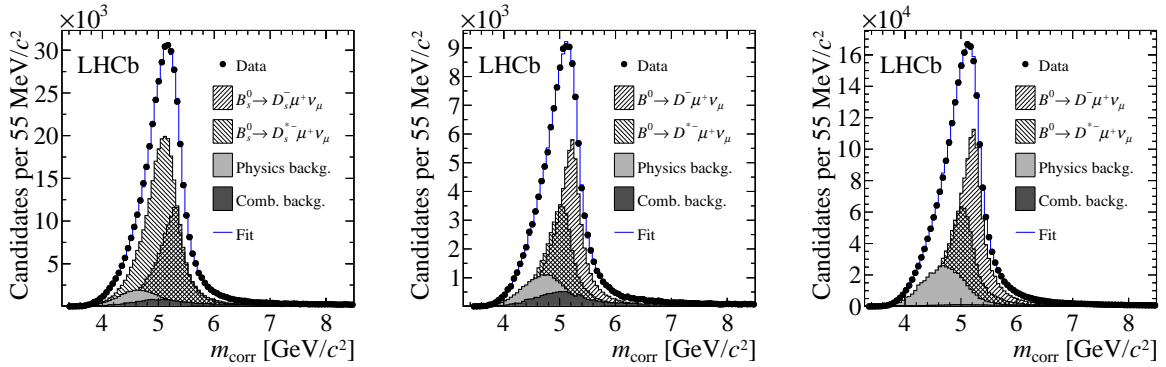


Figure 4: Corrected mass plot for (left panel)  $B_s^0$ , (middle panel)  $B^0 \rightarrow [K^+ K^- \pi^-]_{D^{(*)-}} \mu^+ \nu_\mu$ , and (bottom panel)  $B^0 \rightarrow [K^+ \pi^- \pi^-]_{D^{(*)-}} \mu^+ \nu_\mu$  candidates, with fits overlaid.

Table 1: Results of the fit to the corrected  $B_s^0$  mass distribution. Uncertainties are statistical only.

Component	Fit fraction [%]
$B_s^0 \rightarrow D_s^- \mu^+ \nu$	$29.20 \pm 0.52$
$B_s^0 \rightarrow D_s^{*-} \mu^+ \nu$	$57.77 \pm 0.91$
$B_s^0 \rightarrow D_{(s)}^{(**)} (\rightarrow \mu \nu_\mu) X$	$3.21 \pm 0.74$
$B_s^0 \rightarrow D_s (\rightarrow K \mu \nu_\mu) \tau \nu_\tau$	$4.00 \pm 0.28$
Comb. backg	$5.82 \pm 0.13$

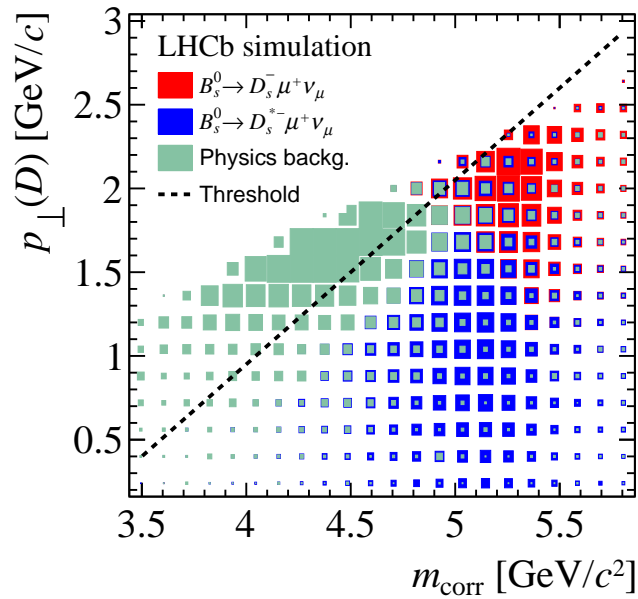


Figure 5: Distribution of the classes of simulated events in the two-dimensional plane of the  $D$  momentum component perpendicular to the  $B$  meson flight direction versus corrected mass. The region accepted in our selection is below the dashed line.

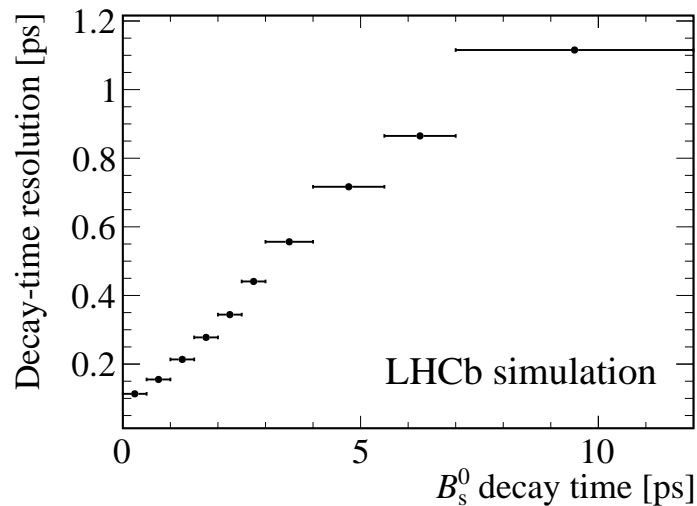


Figure 6: Decay-time resolution as a function of the  $B_s^0$  decay time for  $B_s^0 \rightarrow [K^+ K^- \pi^-]_{D_s^{(*)}} \mu^+ \nu_\mu$  decays.

Table 2: Results of the fit to the corrected  $B^0$  mass distribution of the  $B^0 \rightarrow [K^+K^-\pi^-]_{D^{(*)}-\mu^+\nu_\mu}$  and  $B^0 \rightarrow [K^+\pi^-\pi^-]_{D^{(*)}-\mu^+\nu_\mu}$  samples. Uncertainties on the branching ratios of the decays are included in the expected fractions. The  $B^0 \rightarrow D^-\tau^+\nu_\tau X$  component is shown in parenthesis because it is neglected in the fit to the  $B^0 \rightarrow [K^+K^-\pi^-]_{D^{(*)}-\mu^+\nu_\mu}$  sample. The “prediction” refers to the composition of a sample simulated using form-factors parametrized following Nucl. Phys. **B530** (1998) 153 [arXiv:hep-ph/9712417], with numerical values taken from the *Heavy Flavor Averaging Group* [arXiv:1612.07233], and passed through the analysis selection. Uncertainties are statistical only.

Component	$K^+K^-\pi^-$		$K^+\pi^-\pi^-$	
	Fit fraction [%]	Prediction [%]	Fit fraction [%]	Prediction [%]
$B^0 \rightarrow D^-\mu^+\nu_\mu$	$45.39 \pm 0.67$	$45.83 \pm 3.04$	$49.17 \pm 0.53$	$50.47 \pm 3.05$
$B^0 \rightarrow D_s^-\mu^+\nu_\mu$	$31.16 \pm 0.92$	$32.57 \pm 0.99$	$31.24 \pm 0.93$	$35.10 \pm 0.96$
$B^0/B^+ \rightarrow D^{(**)-}\mu^+\nu_\mu X$	$13.46 \pm 0.47$	$10.83 \pm 1.90$	$15.96 \pm 1.22$	$11.27 \pm 1.90$
$B^0 \rightarrow D^-\tau^+\nu_\tau X$	$(-1.1 \pm 0.9)$	$0.78 \pm 0.22$	$1.26 \pm 0.77$	$0.79 \pm 0.21$
Comb. backg.	$9.99 \pm 0.33$	–	$2.37 \pm 0.07$	–

Table 3: Summary of uncertainties.

Source	Uncertainty on $\Delta_\Gamma(D)$ [ $\text{ps}^{-1}$ ]	Uncertainty on $\Delta_\Gamma(B)$ [ $\text{ps}^{-1}$ ]
Fit bias	0.0004	0.0009
$B_s^0 \rightarrow D_s^{*-}$ decay model	0.0005	0.0025
Sample composition	0.0007	0.0005
$B^0$ -to- $B_s^0$ $p_T$ differences	0.0018	0.0028
Decay-time acceptance	0.0049	0.0004
Decay-time resolution	0.0039	0.0004
$B_c^+$ feed-down	–	0.0010
Total systematic uncertainty	0.0065	0.0041
Statistical uncertainty	0.0117	0.0053